CSMA 2017
13ème Colloque National en Calcul des Structures
15-19 Mai 2017, Presqu'île de Giens (Var)

Numerical simulation of continuous damage and fracture in metal-forming processes with 3D mesh adaptive methodology

F.T. Yang[1], A. Rassineux[1], C. Labergere[2], K. Saanouni[2]

[1] *Sorbonne Université, Université de Technologie de Compiègne, UMR CNRS/UTC 7337, fangtao.yang@utc.fr*
[2] *Université de Technologie de Troyes, ICD/LASMIS, UMR STMR 6279, carl.labergere@utt.fr*

Abstract — An h-adaptive methodology dedicated to the simulation of cracked structures due to the ductile damage is proposed. Cracks are represented using a procedure based on fully damaged elements deletion. Element size inside the domain is driven by size indicators based on plasticity and damage variable. A local remeshing based on a 3D bisection technique and local surface mesh enhancement are applied at a low computational cost. A hybrid field transfer operator is used to keep consistency after remeshing. The loading sequence is also adapted in order to control element deletion.
Key words — adaptive mesh, local remeshing, element deletion, field transfer.

1 Introduction

When a metallic part is formed by large plastic (or viscoplastic) strains, ductile damage is expected to occur inside zones where the plastic flow is highly localized. When ductile damage occurs, the propagation of macroscopic cracks induces severe changes of topology and frequent remeshing must be performed in order to avoid large mesh distortion or element entanglement encountered in a Lagrangian formulation. Our work is focused on meshing and remeshing aspects. In this context, a number of methods have been proposed to represent ductile cracks occurring inside zones where the plastic flow localizes, such as nodal relaxation and cohesive elements [9], element deletion procedures associated with a critical damage criterion [3][5], enrichment techniques such as the extended finite element method (XFEM) [8] based on the addition of an enriched basis into an existing finite element mesh. The present work deals with the prediction of ductile fracture in metal forming where large inelastic (plastic or viscoplastic) strains take place. A fully adaptive scheme which combines size indicators, element deletion, local remeshing, field transfer operators and an adaptive loading sequences technique is used. Various methods [3][6] mostly in 2D and based on finite element have been proposed to predict the ductile fracture occurrence inside metallic parts formed by large plastic deformation based on damage-induced loss of stiffness together with mesh adaptation. As very few techniques have been proposed in a 3D context, we focus on this topic.

2 Mesh adaptation methodology

The FEM based numerical simulation of forming processes involving large inelastic (plastic or viscoplastic) deformations requires adequate spatial discretization of the deformed parts. Indeed, during Lagrangian-based numerical simulations of forming processes, frequent remeshing is needed during the computation in order to avoid large mesh distortion and also to describe the large gradient of the highly localized physical filed, such as damage. The size of the mesh must be driven by appropriate size indicators based both on physical fields (stress, plastic strain, damage ....) and also on the curvature of the external boundary of the domain allowing an accurate enough descritization during the initial step. In our work, the crack is represented by deleting totally damaged elements. Nodal variables such as velocity are transferred by a classical shape function interpolation. All the cumulative integration variables related to the model, such as stresses, plastic strain and damage are transferred from the deformed mesh (old mesh) to the adapted mesh (new mesh) by an enhanced hybrid transfer operator. ABAQUS® is used as an

explicit solver and damage is described by a model from Hooputra et al. [7]. However, the methodology can be used with any other damage related criterion.

2.1 Size indicator

Our methodology is based on the empirical assumption that ductile material behavior can be described by several continuous phases, such as : pure elastic zone without plasticity, homogeneous plastic zone with low damage values, localized plastic zone with moderate damage values and highly localized plastic zone with severe damage values. The mesh size is then mainly driven by the evolution of plastic flow and damage variable. In each of the behavior phase, cumulative plastic strain or damage value can be associated with the mesh size by empirical size indicators detailed in table 1.

TABLE 1 – Empirical size indicators

Behavior phases	Evolution of plasticity p and Damage D	Size indicators
Pure elastic	$p = 0$	$h^p = h_{max}$
Homogeneous plastic	$p \leq p^*$	$h^p = \frac{(h^p_{max} - h_{max})}{p^*} p + h_{max}$
Localized plastic	$p > p^*$	$h^p = (h^p_{min} - h^P_{max})(1 - e^{-\kappa_1 (p - p^*)}) + h^P_{max}$
Moderate damage	$D_{min} < D \leq D_{max}$	$h^D = (h^D_{min} - h_p)(1 - e^{-\kappa_2 (D - D_{min})}) + h^D_{max}$
Severe damage	$D > D_{max}$	$h^D = h^D_{min}$

In table 1, cumulative plastic strain is denoted as p and damage value is denoted as D. A threshold value satisfying a given criterion which maximizes the value of the second invariant of the Cauchy stress is denoted as p^*. Two parameters κ_1 and κ_2 are tuned to minimize the number of elements while capturing the gradient of the physical fields as accuracy. The empirical size indicators are illustrated in figure 1.

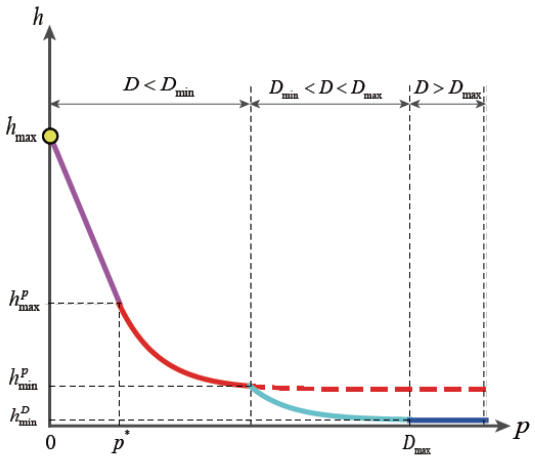

FIGURE 1 – Empirical size indicators

2.2 Local remeshing

A bi-section technique [2] is applied to refine the 3D tetrahedral mesh according to the empirical size indicator as well as to avoid entanglement during large deformation. A background octree is built to keep the size information. An edge of the mesh is split if its length is bigger than the information size obtained from the background octree. An element is then refined if at least one of its edge is determined to be split. The subdivision process is based on the determination of pre-calculated tetrahedron subdivision patterns, as illustrated in Figure 2. We experienced that element shape optimization is needed in a last step. The whole remeshing process including quality optimization is very quick and its computational cost can be neglected compared to the explicit solver. The overall splitting process can be iterated to reach the

prescribed mesh size if needed. Since the process is based on subdivision, much attention should be paid to the initial mesh. The size ratio between adjacent elements should not exceed 2 what limits the creation of ill-shaped elements.

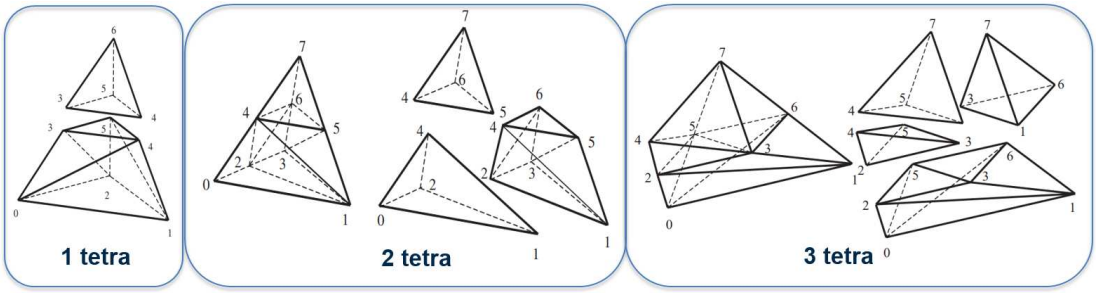

FIGURE 2 – Tetrahedron subdivision patterns

2.3 Field Transfer

After element deletion and mesh adaptation, the topology of the mesh is changed. Therefore, the related variables at both nodal points and integration points should be transferred from the old mesh to the new mesh. The variables at nodal points are transferred by a classical finite element shape function interpolation [9]. The variables at integration points are transferred by a hybrid transfer operator. This hybrid transfer operator is consisted of two steps. In a first step, variables at the integration points of the old mesh are transferred to nodes of the new mesh by Diffuse Interpolation with enhanced point selection. In a second step, these variables are transferred again to integration points of the new mesh by FE shape functions interpolation. This enhanced hybrid transfer has the advantages to deal with problems in which the cumulative physical fields have high gradients and therefore the adapted mesh has a corresponding high gradation. We then focus on the first step.

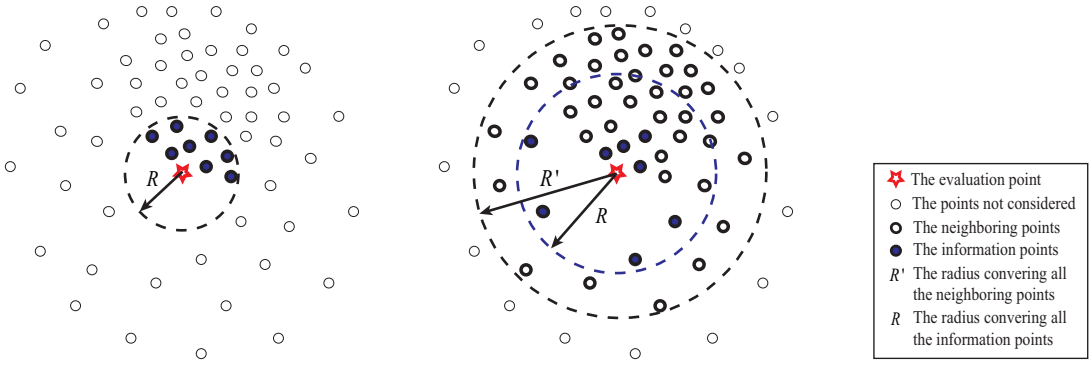

(a) distance Based selection (b) distance/direction Based selection

FIGURE 3 – Information points seletion

Diffuse Interpolation is based on the classical Diffuse Approximation method but in its interpolation form. The selection of the points denoted as information points which are used to build the approximation has been enhanced. Classical information point selection is based only on the distance [3] between neighboring points and the evaluation point. In a 3D tetrahedral mesh context, the number of the neighboring points can be huge up to 400. However, we experienced that no more than 20 points are necessary to build a linear Diffuse Interpolation, otherwise there is too much numerical diffusion [4]. The distance based selection cannot limit the number of the information points. Furthermore, as shown in Figure 3(a), even if the number of points may build the interpolation, the selected set of information points cannot capture the gradient of the fields in some directions. This occurs in areas where mesh gradation is stiff. Therefore, selection of information points must consider both distance and direction in order to capture the gradient of the physical field with accuracy while minimizing numerical diffusion as illustrated in Figure 3(b). In our enhanced information point selection process, for each evaluation point (nodal point

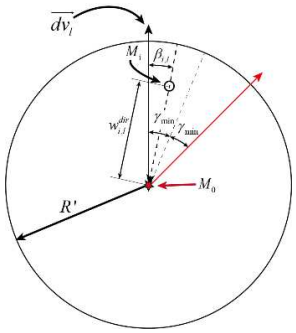

FIGURE 4 – Variables related to the construction of direction weight

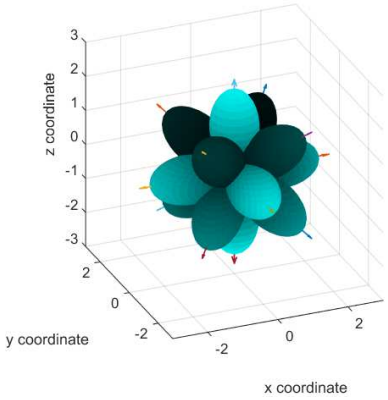

FIGURE 5 – The shape of effective direction weight function

of the new mesh), an element of the old mesh containing the point is determined. All the integration points of the elements which are connected to this containing element are searched as neighboring points using mesh connectivity in order to satisfy a visibility criterion [1]. These neighboring points are then sorted by their relative positions to the evaluation point. A group of information points are then selected from these neighboring points which are distributed the most isotropically around the evaluation points in terms of radial direction. Diffuse Approximation method is then applied in its interpolation form [2] to get the value at evaluation point through the values at the information points. The method to guarantee isotropic distribution of information points as well as limit their number is detailed thereafter.

$$\begin{cases} w_{i,l}^{dir}(M_i, \overrightarrow{dv_l}) = \dfrac{cos(\beta_{i,l}) - cos(\gamma)}{1 - cos(\gamma)}, & \text{if } cos(\beta_{i,l}) \geq cos(\gamma) \quad (1a) \\ 0, & \text{otherwise} \quad (1b) \end{cases}$$

$$\widetilde{w}_{i,l_i^*}^{dir} = max(w_{i,l}^{dir}) \mid_{l=1}^{q} \quad (2)$$

$$w_{i,l}^{dir} = \widetilde{w}_{i,l_i^*}^{dir} \cdot w_i^{\infty} \quad (3)$$

In a first step, a group of referenced direction vectors $\overrightarrow{dv_l}$ which provides an isotropic distribution around the evaluation point M_0 is considered. For each neighboring point, a group of direction weights $w_{i,l}^{dir}$ associated to these direction vectors is constructed, as expressed in Equation (1). The variables used in Equation (1) are defined in Figure 4. In a second step, the effective direction weight $\widetilde{w}_{i,l_i^*}^{dir}$ of each neighboring point is calculated by Equation (2) in which l_i^* is denoted as the number of the direction vector in terms of which direction weight is the maximum one for this neighboring point. The shape of effective direction weight functions with 14 referenced direction vectors is illustrated in Figure 5. In a final step, the effective direction weight and a distance weight w_i^{∞} [3] are combined to form a selection weight. The selected information points are the neighboring points which maximized the selection weight in vicinity of each referenced direction vector. Therefore, the number of final selected information points are linked to the number of referenced direction vectors.

2.4 Results and conclusion

The methodology is validated through the simulation of a tensile test on an aluminum alloy plate specimen (EN AW-7108 T6). The thickness of the specimen is $0.5mm$ and the other dimensions are given in Figure 6. A model from Hooputra et al. [7] is used to describe the damage and ABAQUS® explicit is used as a solver. The left extreme of the specimen is fixed and a constant velocity $2.5mm/s$ is applied at the right extreme. A 10-node tetrahedral (C3D10M in ABAQUS®) is used to perform the simulation. At the very beginning, a coarse mesh is used and the size of the elements are adapted with respect to the curvature of geometry boundary. The evolution of damage is displayed in Figure 7 with the initiation and propagation of the crack. In order to allow the mesh gradation to capture the gradient of the physical

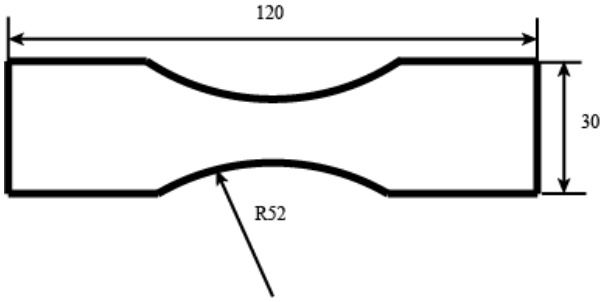

FIGURE 6 – Dimension of the specimen in *mm*

field, the length of the loading sequence should be reduced when plasticity accumulates quickly as shown in Table 2 from loading sequence 1 to 8. If the damage accumulates slowly, the loading sequence can be increased as shown in Table 2 from loading sequence 21 to 28. As a result, at each loading sequence, the increase of the number of the elements is controlled. we can also see that the computational time of the adaptive process including remeshing and field transfer can be neglected compared to the time spent in the solver.

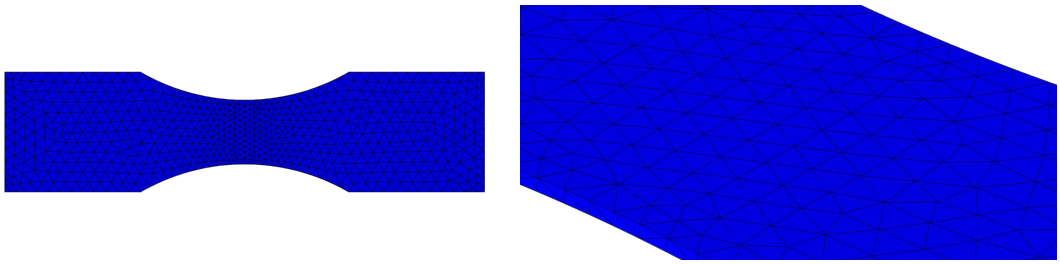

(a) The initial condition

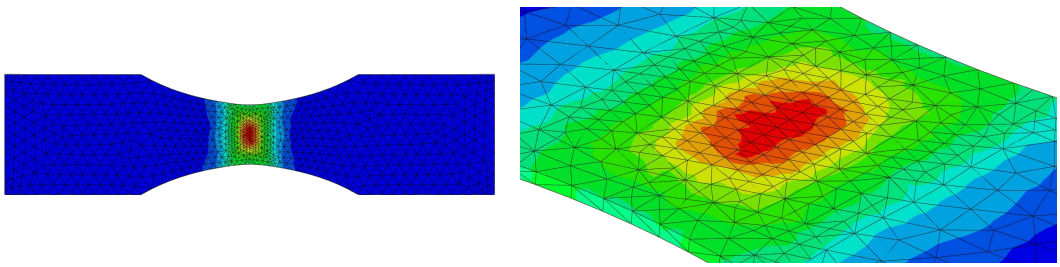

(b) Loading sequence 1

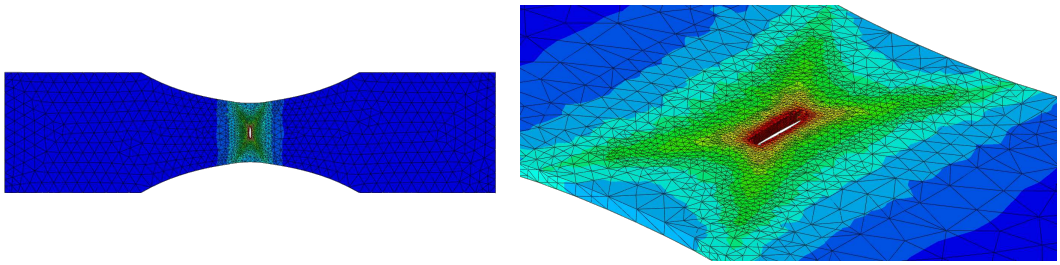

(c) Loading sequence 8

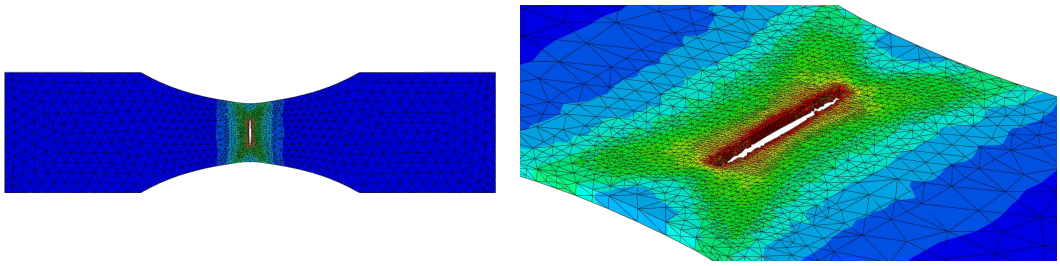

(d) Loading sequence 15

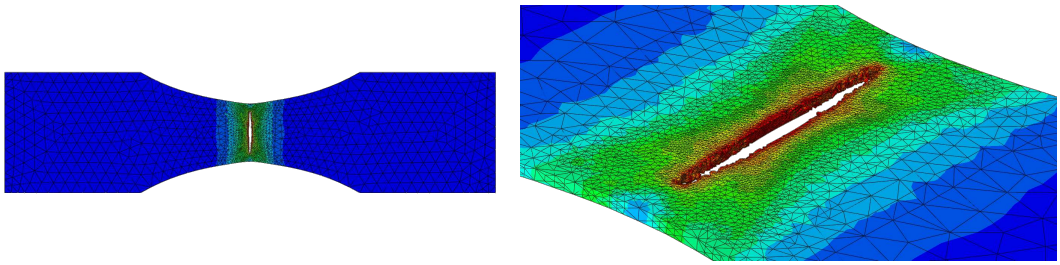

(e) Loading sequence 22

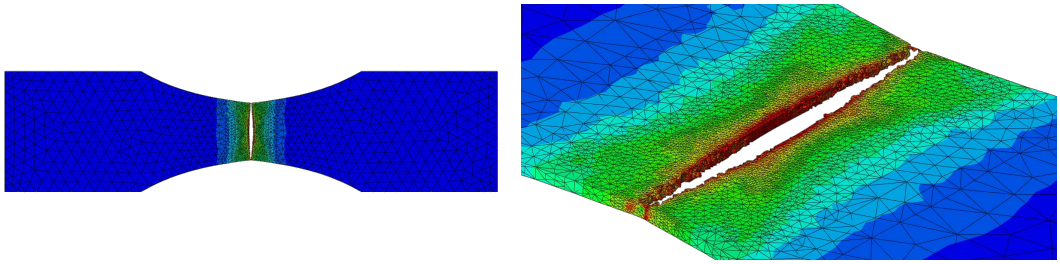

(f) Loading sequence 29

FIGURE 7 – Initiation and propagation of the crack

TABLE 2 – Information of h-adaptive process

Loading sequence	Number of vertex nodes	Number of elements	CPU time of solver (*min*)	CPU time of remeshing (*min*)	Length of loading sequence (*s*)
1	1392	3774	92	<1	1,0000
2	1996	6138	58	<1	0,5000
3	3618	13642	17	<1	0,0500
4	9449	42933	41	<1	0,0300
5	17697	85802	32	<1	0,0200
6	20257	98410	2	<1	0,0010
7	21395	103782	3	<1	0,0010
8	22418	108710	2	<1	0,0005
9	23707	115079	2	<1	0,0005
10	25067	121846	2	<1	0,0005
11	26009	126435	2	<1	0,0005
12	26967	131135	2	<1	0,0005
13	27623	134230	2	<1	0,0005
14	28389	137857	3	<1	0,0005
15	29158	141285	4	<1	0,0005
16	31522	153197	4	<1	0,0005
17	38033	187177	4	<1	0,0005

continued on next page

continued from previous page					
Loading sequence	Number of vertex nodes	Number of elements	CPU time of solver (*min*)	CPU time of remeshing (*min*)	Length of loading sequence (*s*)
18	40625	200003	4	<1	0,0005
19	41989	206539	4	<1	0,0005
20	43134	212172	4	1	0,0005
21	43898	215793	4	1	0,0005
22	44381	218044	6	1	0,0010
23	44834	220223	52	1	0,0100
24	45087	221432	107	1	0,0200
25	45746	224462	263	2	0,0500
26	46531	228255	107	3	0,0200
27	47807	234557	120	1	0,0200
28	49159	241041	136	1	0,0200
29	49839	243977	21	3	0,0050

Reference

[1] A. Rassineux, P. Villon, J-M. Savignat, O. Stab. *Surface remeshing by local Hermite diffuse interpolation*, International Journal for Numerical Methods in Engineering, Wiley Online Library, 31–49, 2000.

[2] A. Rassineux, P. Breitkopf, P. Villon. *Simultaneous surface and tetrahedron mesh adaptation using mesh-free techniques*, International Journal for Numerical Methods in Engineering, Wiley Online Library, 371–389, 2003.

[3] C. Labergere, A. Rassineux, K. Saanouni. *Numerical simulation of continuous damage and fracture in metal-forming processes with 2D mesh adaptive methodology*, Finite Elements in Analysis and Design, Elsevier, 46–61, 2014.

[4] D. Perić, Ch. Hochard, M. Dutko, D.R.J. Owen. *Transfer operators for evolving meshes in small strain elasto-placticity*, Computer Methods in Applied Mechanics and Engineering, Elsevier, 331–344, 1996.

[5] H. Borouchaki, P. Laug, A. Cherouat, K. Saanouni. *Adaptive remeshing in large plastic strain with damage*, International journal for numerical methods in engineering, Wiley Online Library, 1–36, 2005.

[6] H. Borouchaki, P. Laug, A. Cherouat, K. Saanouni. *Aspects of ductile fracture and adaptive mesh refinement in damaged elasto-plastic materials*, International journal for numerical methods in engineering, Wiley Online Library, 29–54, 2001.

[7] H. Hooputra, H. Gese, H. Dell, H. Werner. *A comprehensive failure model for crashworthiness simulation of aluminium extrusions*, International Journal of Crashworthiness, Taylor & Francis, 449–464, 2004

[8] N. Moës, T. Belytschko. *Extended finite element method for cohesive crack growth*, International journal for numerical methods in engineering, Elsevier, 813–833, 2002.

[9] P.O. Bouchard, F. Bay, Y. Chastel, I. Tovena. *Crack propagation modelling using an advanced remeshing technique*, Computer methods in applied mechanics and engineering, Elsevier, 723–742, 2000.